Research article

SURFACE and INTERFACE ANALYSIS

Received: 17 April 2014 Revised: 15 September 2014 Accepted: 25 September 2014 Published online in Wiley Online Library

(wileyonlinelibrary.com) DOI 10.1002/sia.5689

Surface characterization of untreated and hydro-thermally pre-treated Turkey oak woods after UV-C irradiation

Luigi Todaro,[a]* Maurizio D'Auria,[b] Fausto Langerame,[b] Anna Maria Salvi[b] and Antonio Scopa[a]

The aim of this study was to determine the effect of UV-C irradiation on the Turkey oak wood surface (*Quercus cerris* L.). In order to compare the effect of irradiation, both untreated wood samples and those treated with steam and heat were analyzed. The steam treatments were carried out in an autoclave at 130 °C; samples were then heated in an oven for 2 h at 180 °C. The physical and chemical changes brought about in the untreated and treated wood samples by the UV-C light were monitored by colorimetry (color changes), X-ray photoelectron spectroscopy (XPS), Fourier transform infrared spectroscopy (FTIR) (chemical composition) and scanning electron microscopy (SEM) (microstructure and morphology). A detailed analysis of the results indicates that the UV-C treatment caused irreversible changes in both the chemical composition and morphology of the wood samples via photo-oxidation and photodegradation processes. Depending on the type of pre-treatment used, these processes affected the wood samples differently. Copyright © 2014 John Wiley & Sons, Ltd.

Keywords: wood treatment; UV-C irradiation; surface analysis; degradation

Introduction

Wood is widely recognized as the most frequently used construction material due to its structural and aesthetical properties. However, its biological nature makes it susceptible to weathering, which alters its intrinsic characteristics.[1,2]

Weathering can be readily verified by monitoring the color of the wood surfaces.[3] When wood was exposed to ultra-violet (UV) light, water, oxygen or variations in temperature, these factors change the main structure of the wood.

The UV component of sunlight is able to depolymerize components in the cell wall of wood, such as lignin. Lignin and some polysaccharides are the most susceptible components to weathering.[4–9] In addition, weathering accelerates other forms of wood degradation, such as mildew and decay. All these forms of degradation alter the properties of wood, thus affecting the lifetime and usability of products made from wood.[2]

Ultraviolet (UV) radiation is the component of solar light that naturally reaches Earth, and it is classified into one of three categories depending on its wavelength: UV-A (315–390 nm), UV-B (280–315 nm) and UV-C (100–280 nm). Among these, UV-C radiation is the lowest in wavelength, the highest in energy[2] and the most damaging of all three types of UV radiation. Anyway, the UV-C irradiation is mainly a surface treatment so that the eventual damage is only superficial and easy to remove.

However, based on the literature search, the information on the response characteristics of the degradation in natural materials, like wood, on the UVC-induced degradation, remains unsolved.

Recently, several research centers have been active in developing strategies, such as chemical and hydrothermal treatment, to protect wood from weathering and photodegradation.[10] As suggested by Inari *et al.*[11] and Liu,[12] several methods that have been used to analyze the effects of such treatments to photostabilize wood. These methods include assessing (*i*) changes in color using spectrophotometry techniques, such as CIELAB parameters, (*ii*) changes in the chemical composition of the wood using FTIR,[13] Raman spectroscopy,[14,15] and CP-MAS ^{13}C-NMR spectroscopy and[16] (*iii*) the erosion of the wood surface exposed to natural or artificial accelerated weathering using the confocal profilometry technique.[12]

In this study, FTIR and XPS were used to analyze the chemical structure of Turkey oak wood (*Quercus cerris* L.) before and after exposure to hydrothermal treatments (steam and heat) and artificial light (UV-C).

FTIR analysis allowed for the determination of the modifications made to the chemical components contained in the wood, while XPS was employed for the investigation of the surface composition of the wood samples. Given the role that surfaces play when materials are exposed to environments, surface composition can differ from bulk composition.[17–19,11,20,21]

Although conventional XPS might be limited in its ability to resolve chemical groups that are close in energy (e.g. the lipophilic extractives contained in wood)[19] on curve-fitting procedures for spectral elaboration have been widely used for the investigation of wood surfaces[11,20,22] and have provided valuable information on surface chemistry.

* *Correspondence to: Luigi Todaro, School of Agricultural, Forestry, Food and Environmental Sciences, University of Basilicata, Viale dell'Ateneo Lucano, 10, 85100 Potenza, Italy.*
E-mail: luigi.todaro@unibas.it

a *School of Agricultural, Forestry, Food and Environmental Sciences, University of Basilicata, Viale dell'Ateneo Lucano, 10, 85100 Potenza, Italy*

b *Department of Science, University of Basilicata, Viale dell'Ateneo Lucano 10, 85100 Potenza, Italy*

The chemical composition of wood varies with species. Each structure within Turkey oak wood is comprised of different chemical components as evidenced by the extractive compounds present in the heartwood and sapwood components (inner and surface, respectively).[23,24]

Turkey oak wood is an important resource for local micro-economies. In order for it to live up to its potential, it must be pre-treated using heat or water. Attention has been focused on its defects: low dimensional stability, elevated internal tension and low durability. Its introduction in the furniture market has been precluded because it is difficult to glue[25] and has an unappealing surface color.[25] In fact, Turkey oak is less appreciated than other oak species because of its chromatic variations (white sapwood and dark grey heartwood),[25] which are frequently accompanied by the presence of stains and heartwood discoloration (black-heart). However, these stains can be reduced by working the wood in wet conditions or steaming it at high-temperature.[26,27,25] In addition, hydrothermal treatment can lead to a reduction in the moisture content at equilibrium, improving dimensional stability and homogenizing the color.[27,28] This type of oak is used primarily for generating energy (i.e. firewood). However, further information on the characteristics and performance of this material is needed because it is one of the most widely distributed species in Southeast Europe, reaching to Southwest Asia.

Problems caused by hydrothermal treatments, such as surface inactivation,[29] which causes gluing difficulties, remain unresolved and require further investigation. In addition, thermal treatment modifies some characteristics of the wood surface, such as its wettability. Therefore, the improvement of the knowledge in this field is essential for optimizing different wood materials used in industrial processes.

To accelerate degradation phenomena on the wood surface, the most energetic ultraviolet radiation was selected. This paper represents the first study on the possible implications of UV-C irradiation on modified Turkey oak wood surfaces. FTIR and XPS were used to analyze the chemical structure of Turkey oak wood surfaces before and after exposure to hydrothermal treatments (steam and heat) and artificial light (UV-C). Furthermore, a scanning electron microscopy (SEM) was used for morphological and microscopic structural analysis. These analytical multi-techniques provide insight into the degradation mechanisms of weathered woods under different treatment conditions.

Experimental

Material

The wood materials used in these experiments were sampled from four trees growing in a high Turkey oak forest (80 years old) located in the Basilicata Region (Southern Italy). Boards were cut radially from the logs, starting at the pith. Then, samples were extracted from these boards with the annual rings tangentially oriented, producing few nonstandard plain sawn specimens.

The samples employed in this study came from wet lumber (55.1% moisture content); thus, any influence of natural drying on their physical characteristics was avoided.[30]

The wood specimens measured 50 × 7 × 180 mm in the tangential, radial and longitudinal directions, respectively. The wood density in its green state was 0.962 g cm^{-1}. Thirty randomly selected samples were used; *i)* control samples (untreated) and *ii)* hydrothermally treated samples were analyzed and compared. Further information can be found in Todaro *et al.*[27]

Steaming process

Wood treatments were performed at 130 °C and 2.7 bar by indirect steaming inside an autoclave (Vapormatic 770/A, ASAL, Italy). An automatic, thermo-regulated and controlled sterilization instrument with vertical charging was used. The autoclave was equipped with a closed stainless steel basket (Ø 240 × 190 mm height), and it was controlled by a microprocessor, which permitted the programming of various times and temperatures (from 100 to 130 °C) (Fig. 1). The sterilization cycle lasted a total of 280 min; the temperature was quickly increased 130 °C (30 min) that was followed by a short stabilization time (10 min). The temperature was slowly decreased from 130 °C to 100 °C (60 min), and then decreased to 50 °C over 180 min. At the end of the steaming process, the samples had a moisture content of 43.3%.

Heat treatment

Before heat treatment, wood samples were dried in an oven (Vismara Associate, Trezzano, Milano, Italy) until its moisture content was 0%, and then thermally treated at 180 °C for 2 h under atmospheric pressure. Two hours was considered enough time to obtain significant variation in the properties of the wood considering the limited sample size.

UV-C chamber

Turkey oak wood samples were irradiated with UV-C light under controlled conditions (20 °C and 65% of RH) using an irradiation chamber (1 × 0.52 × 0.68 m) that was coated with aluminum sheets and equipped with a UV-C lamp (Helios Italquartz G15T8, 15 W, 3.8 J m^{-2} at 1 m).

After irradiation, the wood samples were analyzed, and the results of the pre-treated (ST130-HT180) and untreated wood samples were compared (Table 1).

Color measurement

Colorimeter parameters, according to the CIELAB system, were used to verify modifications in color. Specific parameters (L*, a*,

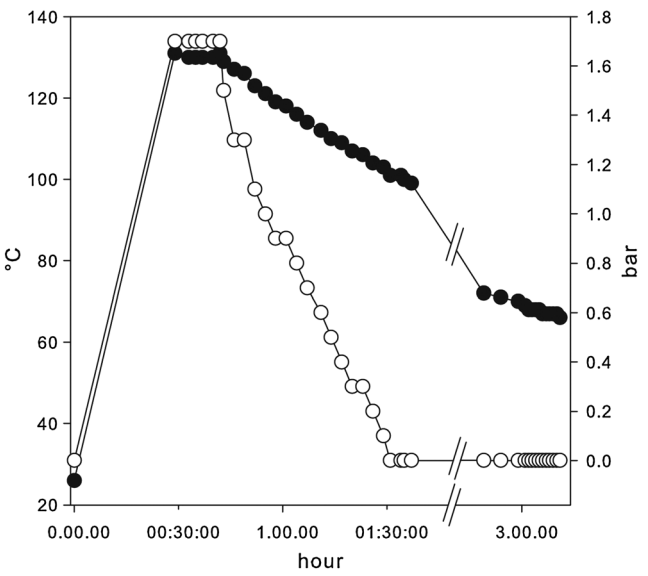

Figure 1. Steaming cycle. (●) is temperature (°C), (○) is pressure (bar).

Table 1. Wood treatments

Treatment code	Steam temp. (°C)	Max pressure (bar)	Heat temp. (°C) (2 h)	UV-C
(a) Untreated (Ctrl)	–	–	–	–
(b) Ctrl + UV-C	–	–	–	x
(c) ST130 + H180	130	2.7	180	–
(d) ST130 + H180 + UV-C	130	2.7	180	x

b*) were measured for each specimen, and their average values were calculated for each treatment. The Minolta CM-2002 spectrophotometer (Minolta Corp, Osaka, Japan) was used. It was equipped with a pulsed Xenon arc light source; the measurement area was 8 mm in diameter. Colorimetric measurements were always performed on the same sample area and repeated 3 times.

The L*, a* and b* values of the specimens were measured before and after the steaming and heating treatments and after the UV-C accelerated weathering test. Color variations (exemplified for ΔL*) were determined according to the following formula:

$$\Delta L = L_{treated} - L_{initial}$$

The ΔL, Δa and Δb values for each sample before and after treatment were also used to calculate the total color change (ΔE) according to the following formula:

$$\Delta E = \sqrt{\left(\Delta L^2 + \Delta a^2 + \Delta b^2\right)}$$

The measurements of color were made at regular irradiation times: 0, 30, 60, 90, 120, 180, 240, 300, 360, 1240, 1400, 2420, 3860, 5300, 6740 and 13940 min.

X-ray photoelectron spectroscopy

XPS spectra were acquired with a LH X1 Leybold (Germany) instrument using a dual achromatic Mg $K\alpha_{(1,2)}$ (1253.6 eV) and Al $K\alpha_{(1,2)}$ (1486.6 eV) source operating at a constant power of 260 W. Wide and detailed spectra were collected using the fixed analyzer transmission (FAT) mode of operation with channel widths of 1.0 or 0.1 eV, respectively, and pass energies of 50 eV. Under these conditions, the instrumental contribution to the line width is kept constant. The measured full width at half maximums (FWHMs) of the Au 4f7/2 (84.0 eV), and Cu 2p3/2 (932.7 eV) signals used for calibration purposes were 1.3 and 1.6 eV, respectively.

The wood samples subjected to different treatments (Table 1) were shaped into rectangles (10 × 7 × 5 mm) so that they would properly fit into the XPS sample holder.

The samples were mounted in the sample holder using double-sided adhesive copper tape, and they were kept under vacuum in the pre-chamber to allow for the vaporization of residual water and/or volatile compounds.

The lengths of the stationary time prior to the analyses were established for all samples by monitoring the pre-chamber pressure. The longest time was required for the highest treated sample, sample d (ST130 + H180 + UV-C). When the final pressure decreased below 10^{-8} mbar, the samples were assumed to be 'degassed' and ready for their transfer into the analysis chamber.

Curve-fitting procedure

The acquired XPS spectra were analyzed using a curve-fitting program (Googly) that has been fully described previously.[31,32] Peak areas were converted to composition in at % using established procedures and the appropriate sensitivity factors (SF).[33] The criteria adopted for data elaboration were based on comparative studies, starting with the analysis of the untreated sample; literature data were referenced[33,34,19,35] and the NIST standard reference database was available online.[36]

In the tables (3 and 4), the peaks in the XPS figures are assigned by reference to the C 1s aliphatic/aromatic carbon (set at 284.8 eV), and the binding energies (BEs) have an overall uncertainty of ±0.2 eV.

The wide spectra were reported as acquired in terms of kinetic energy, whereas the energy scales of the detailed regions were converted to binding energy to facilitate the comparison of the curve fitted results with the literature data.

Fourier transform infrared spectroscopy

Evaluations were conducted on both faces of the samples. Infrared (IR) spectra were obtained utilizing a Bruker Alpha FT-IR spectrophotometer (Bruker Photonics, Billerica, MA) configured for attenuated total reflectance (ATR) at ambient temperature. Spectra from 64 scans were averaged in the range of 400 to 4000 cm^{-1} with 1.0 cm^{-1} resolution.

Environmental scanning electron microscopy

Wood specimens were first trimmed into small blocks. Then, they were cross-cut precisely using a new blade for each surface. The treated and untreated samples, coated with Au thin layer (10 nm), were observed with high vacuum method. A Philips Lab6 environmental scanning electron microscope (SEM) with an energy dispersive X-ray (EDS/EDAX probe) analyzer operating at an acceleration voltage of 20 keV were used.

This instrument was set to a lifetime of greater than 50 s, a CPS (count per second) of ≈2000 and a working distance (WD) ranging from 7.7 to 9.3. Images at different magnifications, acquired by the secondary electrons detector (SE), are reported on the Figs. 6 and 7.

Results and discussion

Color analysis

As indicated in Fig. 2, solid wood samples exposed to UV-C irradiation show, after a small decrease, a stable value of ΔL, which means that both the treated and untreated wood samples become much darker. In all observations of wood color changes using the CIE (L*a*b*) system, the coordinate b* was the most affected for the untreated wood, while Δa varied only slightly. The positive value of Δb means that the untreated wood tends to yellow.

Two phenomena could be distinguished by analyzing the ΔE variation curves (Fig. 2). During the first 2420 min of exposure, a rapid increase was observed for the untreated samples. After this time, the variation tends to stabilize and only a slight decrease is seen after 5300 min. For the treated samples, after an initial increase up to 1400 min, a weak decrease was also obtained. According to Sundqvist and Morén,[37] the human eye can distinguish a color change corresponding to a ΔE as low as 2–3 units. It is important to note that at the end of the exposure the color changes of the two types of wood samples tend is similar.

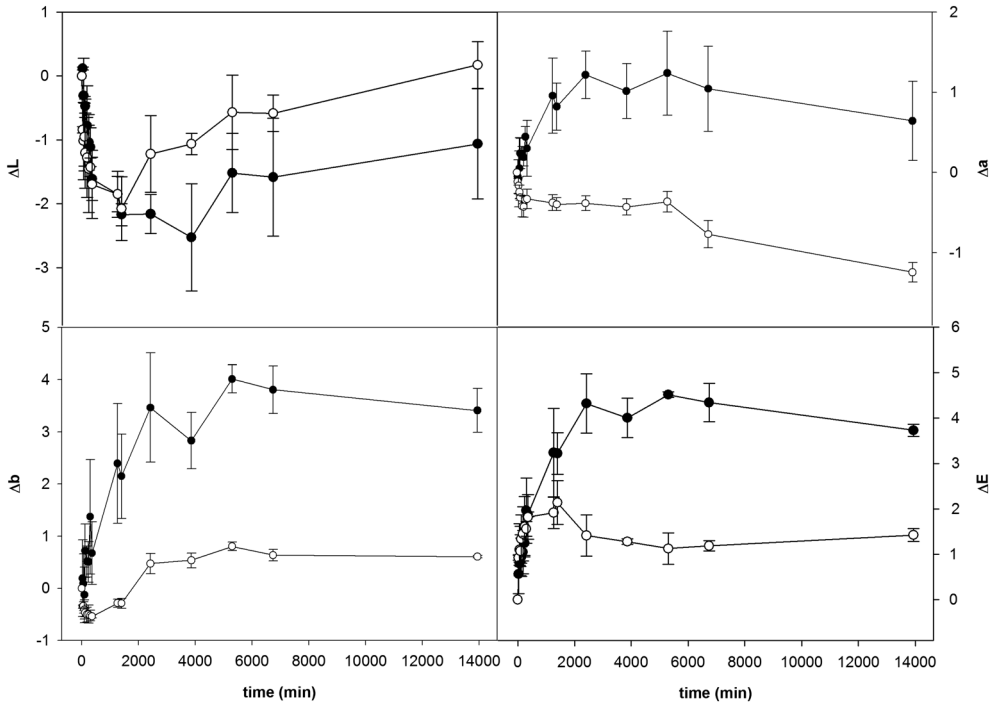

Figure 2. The time evolution of the Cielab coordinates in Turkey oak wood during UV-C irradiation.

The color measurements after steam and heat treatment (Table 2) were derived from previous work by Todaro *et al.*.[27] Here, for treated wood, most of the discoloration (22.5) is noted after the steam treatment step (Table 2). As reported by Sundqvist,[37] these color changes are due primarily byproducts of the hydrolysis of carbohydrates and extractives. Hydrolysis is an important reaction that occurs when wood is heat treated and moisture is present in wood cells or when wood is steamed. The level of moisture in the hardwoods and the temperature used during their drying and steaming have been found to be the most important factors affecting darkening.[28]

The discoloration also depends on the photochemical stability of the lignin and extractives. In fact, the extractive content was 2.9% and 4.1% for the untreated and treated wood samples, respectively.[24] However, thermal treatments that are longer in durations (similar to what is used in industrial applications) and that achieve higher maximum temperatures could change the color even more. In that case, even UV-C radiation could modify the color more significantly, considering that the photons of the UV-C range have sufficient energy to split almost all chemical bonds existing in wood.[38]

After many hours of UV-C irradiation, the treated wood was characterized by a smaller color change than the untreated wood (Table 2). In particular, in the CIELAB color space, both types of samples showed similar brightness values (−1.1 and 0.2 for untreated and treated wood, respectively). In addition, the two curves depicted the tendency of the wood surfaces to darken over time (Fig. 2). Little variation in Δa* (the green–red axis) was observed. The untreated wood samples had higher values while of Δb* (the blue–yellow axis) than the treated samples, and the variations were not constant over time (Fig. 2). Other studies have shown that the color of heat-treated wood was unstable and faded with prolonged exposure to UV radiation.[39,40] The main problem of the untreated Turkey oak wood is the uneven spots present in the surface. For treated wood we observed a slight lower extent for brightness and yellow and slightly higher for red, but the treated samples underwent high variations during the hydrothermal treatment letting to a darkening, loss of yellow and increase of red. However, the low values of the standard deviation of the final ΔE (Fig. 2) in treated wood samples, pointed out that the problem of inhomogeneous of the color could be solved with a previous thermo treatment.

XPS analysis

Untreated sample

Figure 3 and Table 3 show the wide and detailed spectra of the untreated samples with the corresponding curve fitting results.

The wide spectrum shows carbon and oxygen elements, as expected in wood, and nitrogen in a lesser amount. As labeled in the spectrum, the most intense XPS signals (C 1s and O 1s) are

Table 2. Color changes after steam, heat and UV-C treatments

Treatment code	After steaming				After heating				After UV-C			
	ΔL	Δa	Δb	ΔE	ΔL	Δa	Δb	ΔE	ΔL	Δa	Δb	ΔE
(a) Untreated (Ctrl)	_	_	_	_	_	_	_	_	−1.1	0.6	3.4	3.7
(c) ST130 + H180	−21.5	4.1	−4.9	22.5	−7.0	−0.4	−3.4	8.1	0.2	−1.2	−1.2	1.4

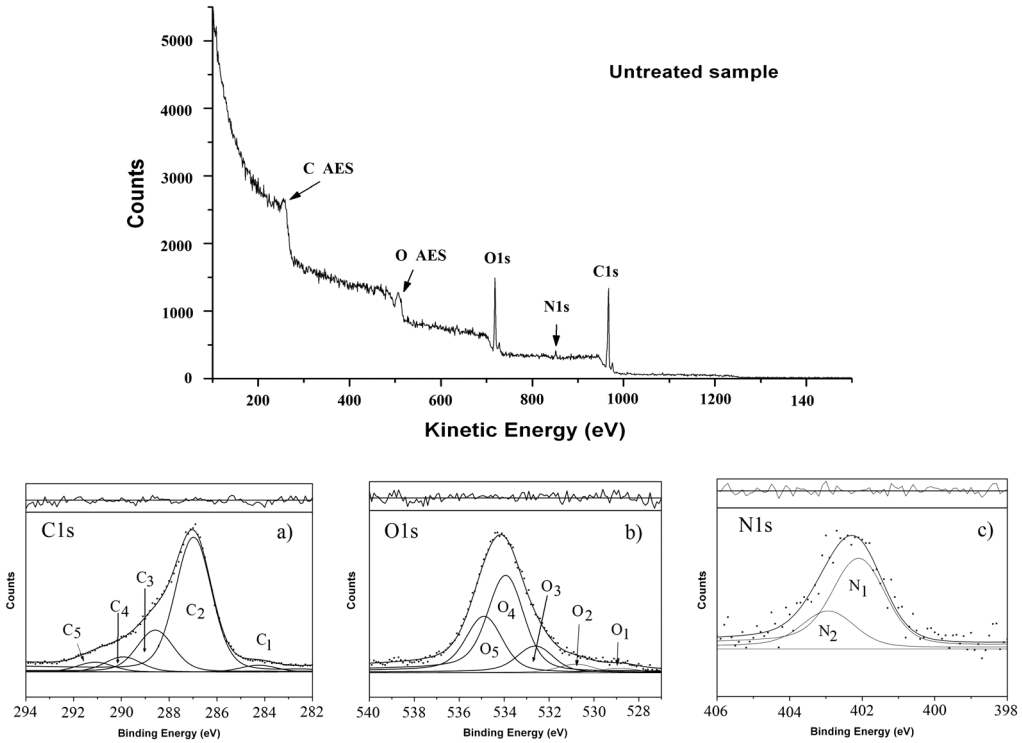

Figure 3. Turkey oak wood. Wide spectrum and C 1s (a), O 1s (b) and N 1s (d) curve-fitted regions.

Table 3. Fitting parameters for the detailed regions in Fig. 3

Element	Peak number	BE corr. (eV)	Corrected area (arbitrary units)	Assignment
C 1s	1	282.1	189.9	
	2	284.8	3748.4	C—C, C—H
	3	286.4	1165.4	C—O, C—OH, C—CN, C=N
	4	287.7	420.6	C=O, O—C—O, CO—NH_2, C—CO—NH—C
	5	289.7	273.6	COOH, C—O—CO—O—C
O 1s	1	527.0	47.9_5	Co(CH_3—(C_5H_3N)—N=N—(C_6H_3)(O)(O))(CH_3—(C_5H_3N)—N=N—(C_6H_3)(O)(OH)).0.5NaCl
	2	529.3	92.4	CH_3—(C_5H_3N)—N=N—(C_6H_3)(OH)(OH)
	3	531.7	271.2_5	C=O
	4	533.1	984.1	C—O—
	5	534.8	572.5	O—CO—O/H_2O
N 1s	1	399.9	95.8	R—CO—NH_2, C—NH_2, —C—CO—NH—C, N—CO
	2	400.7	40.1	R—CO—NR—CO—R

accompanied by their Auger signals (CAES and OAES) arising from the relaxation of the X-ray photoexcited atoms.[33] The detailed spectra were resolved by fitting the curves using certain constraints to ease Googly computation. The procedure was based on the use of the minimum number of peak components, the same FWHMs and shapes within each spectral region, and the 'chi-square' (χ^2) test and visualization of residual excursions (Fig. 4), which were used to judge the goodness of fit. The main components can accommodate closely spaced chemical states as explained below and as the assignments reported in Table 3 indicate.

C 1s region

The C 1s signal was fitted with five peaks (Table 3) (FWHM = 1.8 eV).

The first one (**peak 1**) had the lowest binding energy (282.1 eV) of the carbide species. This peak is not specifically assigned in the table, and it could be related to polymers of the type $(C_6H_5NC_6H_4)_n$ or similar compounds that are reported as 'extractives'. These species are able to migrate from the inside of a wood sample to its surface under ultra-high vacuum (UHV) XPS measurements.[19]

Peak 2 (284.8 eV) results from the emission from carbon singly bonded to either hydrogen or other carbons; it was used for the determination of surface charging (internal standard) and the correction of binding energies. **Peak 3** (286.4 eV) is due to emissions from carbon singly bonded to oxygen and includes nitrogen-containing carbon bonds. **Peak 4** (287.7 eV) results from carbonyl groups, HN—C=O, and/or O—C—O groups. **Peak 5** (289.7 eV) is assignable to carboxylic acids and esters, including C—O—CO—O—C groups.

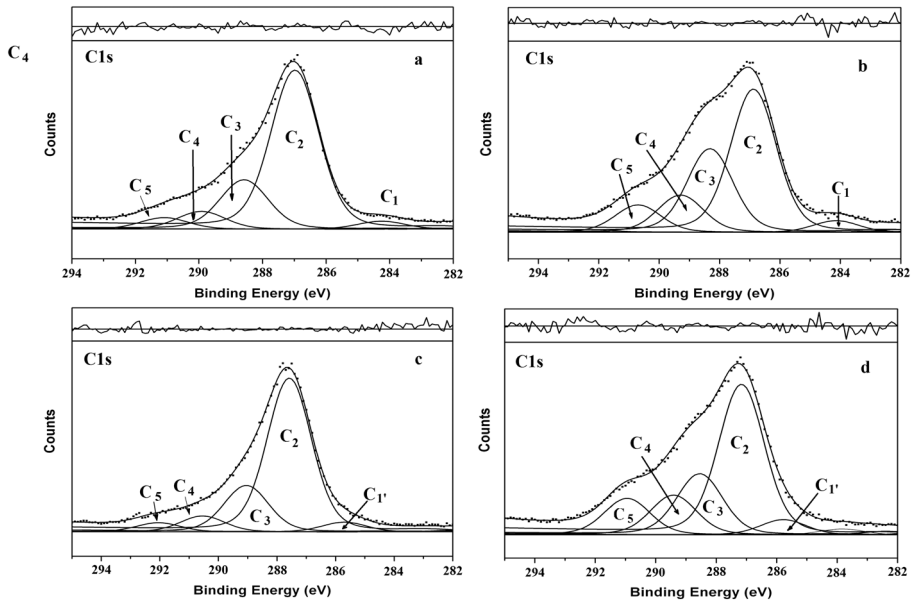

Figure 4. Turkey oak wood samples. C 1s curve-fitted regions: a) untreated sample, b) after UV-C irradiation, c) after steaming and heat treatment and d) after steaming, heating and UV-C irradiation.

O 1s region

The O 1s curve-fitted region is composed of five peaks (FWHM = 2.0 eV) (three main components (O_3, O_4 and O_5) and two components at lower BE (O_1 and O_2)). The lower BE peaks, similar to those in the carbon region, are more difficult to properly identify (see some probable compounds reported in Table 3) and more prone to be affected by wood treatment.

The O_3 peak at 531.7 eV and the O_4 peak at 533.1 eV correspond to carbonyl oxygen and oxygen singly bonded to carbon, respectively. The O_5 peak corresponds to carboxyl/esters or O—CO—O groups as well as the oxygen atoms of strongly confined residual water.

N 1s region

The N 1s peak can be fitted with two components (FWHM = 1.7 eV) belonging to amide/amine groups (**peak 1**, 399.9 eV) and R—CO—NR—CO—R or 'charged' amine groups (**peak 2**, at 400.7 eV) likely with anthropogenic and environmental origins. The amount of nitrogen found in the wood samples was few percent, and it could be due to emission from the nitrogen-containing functional groups of the 'extractives' associated with the lowest BE peaks of the carbon and oxygen regions.

Treated wood

To facilitate the comparison of treated samples (named b, c and d), their C 1s, O 1s and N 1s regions were curve-fitted using the same number of components of the same peak shapes as the untreated sample a. The program adjusted the FWHM to the best value for each spectral region.

Using this simplified approach, the main components may have, depending on the treatment used, a shift in their binding energies compared to those shown in Table 3; however, the major classes of chemical groups were successfully identified. The changes in the relative intensities of the peaks were used to assess the effect of each treatment.

The C 1s curve-fitted regions are more easily resolved than the O 1s regions. The nitrogen content is too low in all samples for those peaks to be distinguished. Therefore, the peak intensities of the C 1s regions were compared following treatment (Fig. 4). In addition, the at % composition, N/C and O/C ratios, and the carbon component distribution of the four analyzed samples were reported (Table 4).

The effect of the treatments on the wood samples could thus be determined by comparing the XPS results of each treated sample with those of each untreated sample.

Regarding the at % composition, carbon is always present at the highest percentage. The N/C and O/C ratios follow a similar trend (Table 4), but given the low amount of nitrogen, the O/C ratio can be more easily followed to assess the effect of a particular treatment.

UV-C irradiation induces carbon oxidation and thus an increase of the O/C ratio by promoting the scission of unsaturated bonds and free radical oxygen reactions. Also, the C_2 (C—C, C—H) signal decreases while that of the oxidized carbons increases: $C_3 > C_4 > C_5$. The carbon with the lowest binding energy is still present as well as the O 1 and O 2 peaks in the curve-fitted O 1s

Table 4. XPS spectral parameters. At % compositions, O/C and N/C ratios, and C_1/C_1', C_2, C_3, C_4 and C_5 distributions of Turkey oak wood after different treatments.

Treatment code	O (%)	C (%)	N (%)	O/C	N/C	C_1/C_1' (%)	C_2 (%)	C_3 (%)	C_4 (%)	C_5 (%)
(a) Untreated (Ctrl)	24.9	73.4	1.7	0.34	0.02	2.4	47.4	14.7	5.3	3.5
(b) Ctrl + UV-C	31.7	65.7	2.6	0.48	0.03	2.5	30.9	18.1	8.1	5.9
(c) ST130 + H180	19.3	79.9	0.8	0.24	0.01	3.3	52.2	15.8	5.4	3.1
(d) ST130 + H180 + UV-C	30.3	67.3	2.4	0.45	0.03	3.4	33.4	13.6	8.8	8.1

region (not shown). The N/C and O/C ratios increase by roughly the same amount within the limit of our accuracy in quantification.[33]

The ST130 and HT180 treatments induce exactly the opposite effect. The C_2 (C—C, C—H) signal increases, while that of the oxidized carbons decreases. Thus, the O/C and N/C ratios decrease. This effect can be attributed to degradation that occurs during thermal treatment[41,34,19,11,35] and induces either a decrease in the amount of hydroxyl groups, the loss of volatile, oxygen-containing 'extractives' or the migration of by-products with a lower oxygen content to the surface.

In sample (c) we see the lower BE carbon (C_1) moved ~1 eV higher (C_1') in the C1s region, the disappearance of O_1 and strong reduction of O_2 in the correspondent O1s region (not shown) and the lowest registered N/C ratio (Table 4).

Sample (d) was subjected to a combined treatment (ST130 + H180). The spectrum of this sample shows an intermediate O/C ratio (Table 4). This intermediate value was obtained because a combination of the effects, mentioned previously, is in play. The disappearance of both the O_1 and O_2 peaks (registered in the O 1s region, not shown) would indicate oxygen-containing volatile compounds departed during heat treatment, lowering the oxygen content. UV-C irradiation followed by ST and HT180 treatments induces a more progressive oxidation that leads to an increase of C_4 (carbonyls) and C_5 (carboxylic and ester-type groups) peaks at the expenses of the C_3 peak (carbon singly bonded to oxygen), thus augmenting the total O/C ratio.

In summary, the absorption of contaminants and biocontaminants from the environment, the migration of non-volatile extractives originating within the sample itself and the evolution and degradation of water and volatile by-products following heat treatment alter the surface composition of wood samples. The treatment increases the C—C and C—H components (C_2) and decreases the O/C ratio in comparison with that estimated for the bulk.

As previously stated,[29] a low O/C ratio and intense C—C and C—H peaks reflect a high concentration of non-polar components (extractives/VOCs) on the wood surface that can reduce its wettability; the surface goes from being hydrophilic to being hydrophobic.

However, oxidation was initiated on the surfaces, and we monitored this reaction and the effect of UV-C irradiation on sample pre-treatment and storage. We have shown that the combined action of steam and heat pre-treatments makes carbon oxidation progress more efficiently under UV-C irradiation, not only reducing C_2 intensity but further oxidizing single C—O— bonds (C_3) into double C=O bonds (C_4) and more oxidized compounds of the C—O—CO—O—C type (C_5).

FTIR analysis

First, the untreated sample was analyzed. The sample (Fig. 5a) showed a signal at 1735.7 cm^{-1}, identified as the carbonyl absorption band of aliphatic aldehydes, ketones and esters. Furthermore, the sample showed absorption bands at 1597.4, 1552.7 and 1513.6 cm^{-1}, which were attributed to aromatic skeletal vibrations. The absorption band at 1468.5 cm^{-1} results from the C—H deformations of methylene and methyl groups.[42]

When the sample was hydrothermally treated (ST plus HT180), we observed a clear shift of the absorption hand of the aliphatic carbonyl groups from 1735.7 to 1743.1 cm^{-1} (Fig. 5b). Furthermore, an increase in the absorption band near 1660 cm^{-1} was observed in agreement with an increase of the presence of conjugated carbonyl groups in the sample. The same types of modifications were observed in the untreated sample when it was exposed to UV radiation (Fig. 5c). Also, a shift of the aliphatic carbonyl absorption band at 1747.9 cm^{-1} and an increase in the conjugated carbonyl region near 1660 cm^{-1} was observed (Fig. 5c). When the hydrothermally treated wood was exposed to UV radiation, few modifications were observed in the FTIR spectrum (Fig. 5d). The treated sample was much more resistant than the untreated sample. A shift from 1743 to 1746.7 cm^{-1} was observed for the absorption band corresponding to the aliphatic carbonyl groups in lignin, while increases were not observed in the conjugated carbonyl region (Fig. 5d). Further, the signals at 1262 (due to the guaiacyl units)[42] and 1462 cm^{-1} decreased.

The same behavior was not observed when European spruce wood was treated with a high pressure xenon arc lamp (>280 nm).[43] In that study, an increase in the signal at 1730 cm^{-1} was observed and a sharp decrease in the aromatic signal at 1510 cm^{-1} was seen. On the contrary, we did not observe an increase in the signal due to the presence of aliphatic carbonyl compounds; we only saw shift for this signal. Further, a reduction of the aromatic signal near 1510 cm^{-1} was not observed. The shift

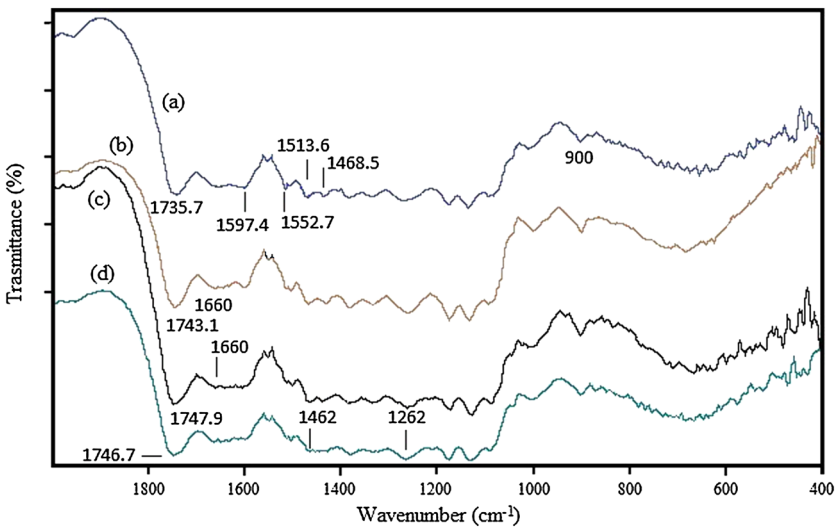

Figure 5. FTIR spectra of Turkey oak wood samples: a) untreated, b) ST130 and HT180, c) untreated and UV-C and d) ST130, HT180 and UV-C.

of the aliphatic carbonyl signal can be explained by considering a relative increase in the signal of the contribution due to the presence of aliphatic acids or esters. The effect is likely due to the oxidation of the aldehyde groups present on both the lignins and carbohydrates.

Finally, after thermal treatment, we observe an increased in the absorption near 900 cm^{-1} that is due to the aromatic C—H out of plane bending. When the untreated sample was treated with UV light, a change in this signal was not induced. When the thermally treated sample was exposed to UV irradiation, a reduction in this signal was observed. The UV treatment of the untreated sample increases the polymerization of lignin, while the UV treatment of the thermally treated sample causes the oxidation of the aromatic skeleton.

SEM high vacuum analysis

The morphology and microstructure of wood samples that were subjected to different treatments were examined by SEM high vacuum method (Figs. 6 and 7). The surface properties of the

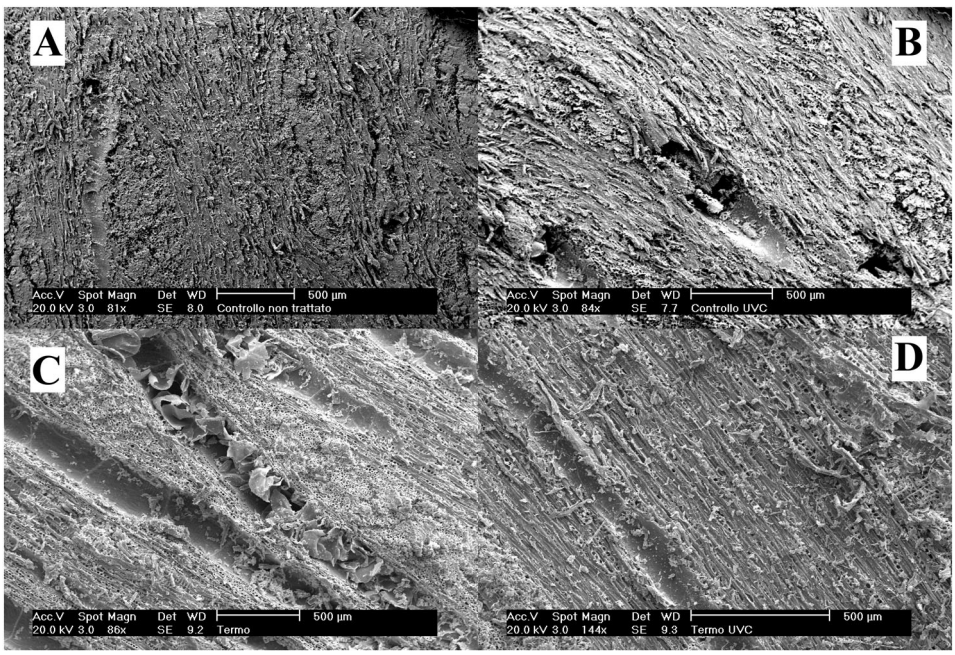

Figure 6. ESEM micrographs of heat-treated Turkey oak wood: (A) control, (B) control and UV-C, (C) ST130 and H180 and (D) ST130, H180 and UV-C.

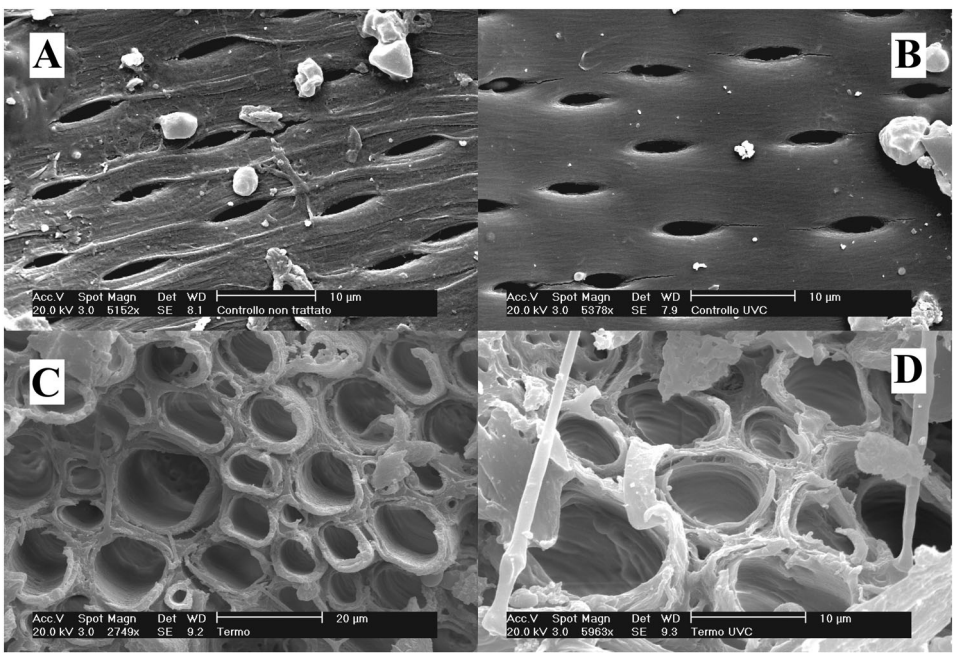

Figure 7. Vessel pits in control (A) and control + UV-C and the modification of multiseriate ray cells due to steam and heat treatment (C) and UV-C effects (D).

steam- and heat-treated wood that was treated UV-C light changed because of the degradation of the chemical constituents of wood and the removal or migration of extractives and other compounds from the wood.

The images showed that the structural integrity of the cellular structures was modified the most in the most severely heat-treated wood sample (ST 130 plus H180). The UV-C treatment caused additional damage, erosion and deterioration of the inside of the inner surface of the vessels (Figs. 6B and 6D).

The most magnified images reveal how the wood develops diffuse modifications of the cell wall layers of the ray parenchyma (Figs. 7C and 7D). These cells were damaged likely because the steam caused some of the structures to plasticize.[24] The thermal treatment might have also caused damage. The vessels and fibers of the tracheids are modified. These changes are likely attributed to plasticization and spurt out of lignin (Fig. 7D). Turkey oak is very sensitive to structural damage during (or after) hydrothermal treatment. As discussed, the heat and steam treatment of green wood[37,25] resulted in chemical changes in the wood samples likely because the hemicelluloses and other components, such as extractives, are degraded.[24]

In contrast, cracks were found in the untreated wood samples that were irradiated with UV-C light (Fig. 7B). The features seen in these microphotographs are related to the inner (lumen) surface of vessels. Tangential fractures were noted around the pit apertures of the untreated wood samples that were irradiated with UV-C light. Detached slivers of wall material were seen in the multiseriate ray cells of the treated wood (Fig. 7C). In addition, evidence of fungal colonization was also seen in treated wood that was subjected to UV-C irradiation (Fig. 7D). This evidence should be better investigated.

Conclusions

In this study we detected the performances of untreated and hydrothermally treated Turkey oak wood to extreme UV-C exposure.

The hydrothermally wood surfaces exhibited better color stability after the UV-C irradiation. For the most part, the color changes were seen by the end of the steaming step, thus the major global color modifications of the wood samples (ΔE) can be observed in the untreated samples. This variation was almost entirely due to variations in Δb^*.

The XPS data showed a decrease in the oxygen content of the wood surface after the hydrothermal treatment, indicating that compositional modifications occurred. After UV-C irradiation, the carbon oxidation of this sample progressed (to higher oxidations states) in comparison to the untreated wood samples.

FTIR data showed, by comparing shifts in carbonyl absorption, conjugated carbonyls and aromatic signals, that UV-C irradiation mainly induces the polymerization of lignin in untreated wood samples and the oxidation of the aromatic skeletons in thermally treated wood samples.

The SEM high vacuum analysis showed that heat treatment induces profound structural modifications in the wood cells; the structure of the wood cells is not further modified by the addition of UV-C irradiation. On the contrary, the cracks were observed in the untreated wood samples after their exposure UV-C irradiation.

Each technique has its own set of characteristics (some sample smaller areas and all have different sampling depths). The results of these different analytical techniques all indicate the same outcome and consistently corroborate the color measurements. In fact, both XPS (surface) and FTIR (sub-surface) reveal an advanced the oxidation state of the chemical components of the treated woods indicative of color degradation. Moreover, SEM high vacuum analysis confirms the structural changes of the hydrothermally treated wood.

Acknowledgements

All authors contributed equally to this work. Thanks to Dr Angelo Rita for graphical assistance, Stefania Vergura, Ernesto Santoro and Mariangela Curcio for their exercises on XPS curve-fitting and experimental reports. The authors gratefully acknowledge the University of Basilicata for the instrumental facilities at CIGAS lab and, especially, Mr. Alessandro Laurita for SEM analyses.

References

[1] D. N. S. Hon, G. Ifju, *Wood Sci.* **1978**, *11*, 118–127.
[2] M. Kutz, *Handbook of Environmental Degradation of Materials*, William Andrew Publishing, Norwich, NY, **2005**.
[3] A. Temiz, N. Terziev, M. Eikenes, J. Hafren, *Appl. Surf. Sci.* **2007**, *253*(12), 5355–5362.
[4] C. Bonini, M. D'Auria, L. D'Alessio, G. Mauriello, D. Tofani, D. Viggiano, F. Zimbardi, *J. Photochem. Photobiol., A.* **1998**, *113*, 119–124.
[5] C. Bonini, M. D'Auria, G. Mauriello, D. Viggiano, F. Zimbardi, *J. Photochem. Photobiol., A.* **1998b**, *118*, 107–110.
[6] G. Buschle-Diller, S. H. Zeronian, in *Photochemistry of lignocellulosic materials* (Eds: C. Heitner, J. C. Scaiano), American Chemical Society, Washington, DC, **1993**, pp. 177–189.
[7] C. Crestini, M. D'Auria, *J. Photochem. Photobiol., A.* **1996**, *101*, 69–73.
[8] C. Crestini, M. D'Auria, *Tetrahedron* **1997**, *53*, 7877–7888.
[9] I. Forsskähl, H. Tylli, in *Photochemistry of lignocellulosic materials* (Eds: C. Heitner, J. C. Scaiano), American Chemical Society, Washington, DC, **1993**, pp. 45–59.
[10] B. M. Esteves, H. M. Pereira, *BioResources* **2009**, *4*(1), 370–404.
[11] G. N. Nguila Inari, M. Pétrissans, S. Dumarcay, J. Lambert, J. J. Ehrhardt, M. Sernek, P. Gérardin, *Wood Sci. Technol.* **2011**, *45*, 369–382.
[12] C. Liu, PhD thesis, University of British Columbia, **2011**.
[13] B. F. Tjeerdsma, H. Militz, *Holz Roh- Werkst.* **2005**, *63*(2), 102–111.
[14] U. P. Agarwal, J. D. McSweeny, S. A. Ralph, *J. Wood Chem. Technol.* **2011**, *31*, 324–344.
[15] S. Yamauchi, A. Koizumi, *Eurasian J. For. Res.* **2009**, *12*(1), 57–63.
[16] B. F. Tjeerdsma, M. Boonstra, A. Pizzi, P. Tekely, H. Militz, *Holz Roh-Werkst.* **1998**, *56*, 149–153.
[17] L. S. Johansson, J. M. Campbell, *Surf. Interface Anal.* **2004**, *36*, 1018–1022.
[18] K. Li, D. W. Reeve, *J. Wood Chem. Technol.* **2004**, *24*, 183–200.
[19] G. N. Nguila Inari, M. Pétrissans, J. Lambert, J. J. Ehrhardt, P. Gérardin, *Surf. Interface Anal.* **2006**, *38*, 1336–1342.
[20] P. Nzokou, D. P. Kamdem, *Surf. Interface Anal.* **2005**, *37*, 689–694.
[21] N. M. Stark, L. M. Matuana, *Polym. Degrad. Stab.* **2004**, *86*(1), 1–9.
[22] M. Sernek, PhD thesis, Virginia Polytechnic Institute and State University, Blacksburg, **2002.**
[23] P. Lavisci, X. Deglise, *Holzforschung* **1991**, *45*(6), 415–418.
[24] L. Todaro, P. Dichicco, N. Moretti, M. D'Auria, *BioResources* **2013**, *8*(2), 1718–1730.
[25] L. Tolvaj, S. Molnár, *Acta Silv. Lign. Hung.* **2006**, *2*, 105–112.
[26] Y. Cao, J. Jiang, J. Lu, R. Huang, J. Jiang, Y. Wu, *BioResources* **2012**, *7*(3), 2809–2819.
[27] L. Todaro, R. Zanuttini, A. Scopa, N. Moretti, *Wood Sci. Technol.* **2012a**, *46*, 563–578.
[28] L. Todaro, L. Zuccaro, M. Marra, B. Basso, A. Scopa, *Wood Sci. Technol.* **2012b**, *46*, 89–100.
[29] M. Sernek, F. A. Kamke, W. G. Glasser, *Holzforschung* **2004**, *58*, 22–31.
[30] L. G. Esteban, J. Gril, P. de Palacios, G. Casasu`s, *Ann. For. Sci.* **2005**, *62*, 275–284.
[31] J. E. Castle, H. Chapman-Kpodo, A. Proctor, A. M. Salvi, *J. Electron Spectrosc. Relat. Phenom.* **1999**, *106*(1), 65–80.
[32] J. E. Castle, A. M. Salvi, *J. Electron Spectrosc. Relat. Phenom.* **2001**, *114–116*, 1103–1113.
[33] D. Briggs, J. T. Grant, *Surface Analysis by Auger and X-ray Photoelectron Spectroscopy*, IM Publications, Chichester, UK, **2003**.

[34] H. Du, W. Wang, Q. Wang, Z. Zhang, S. Sui, Y. Zhang, *J. Appl. Polym. Sci.* **2010**, *118*, 1068–1076.
[35] G. Sinn, A. Reitere, S. E. Stanzl-Tschegg, *J. Mater. Sci.* **2001**, *36*, 4673–4680.
[36] http://srdata.nist.gov/xps/ Last accessed February **2013**
[37] B. Sundqvist, T. Morén, *Holz Roh- Werkst.* **2002**, *60*(5), 375–376.
[38] L. Tolvaj, K. Mitsui, *J. Wood Sci.* **2005**, *51*, 468–473
[39] A. Ahajji, P. Diouf, F. Aloui, I. Elbakali, D. Perrin, A. Merlin, B. George, *Wood Sci. Technol.* **2009**, *43*, 69–83.
[40] T. Syrjänen, E. Kangas, The International Research Group on Wood Preservation, IRG/WP 00-40158, **2000**.
[41] R. Alén, R. Kotilainen, A. Zaman, *Wood Sci. Technol.* **2002**, *36*, 163–171.
[42] O. Faix, in *Methods in Lignin Chemistry* (Eds: S. Y. Lin, C. W. Dence), Springer-Verlag, Berlin, **1992**, pp. 83–109.
[43] U. Müller, M. Rätzsch, M. Schwanninger, M. Steiner, H. Zöbl, *J. Photochem. Photobiol. B* **2003**, *69*, 97–105.